Conformational Analysis of a Highly Potent, Constrained Gonadotropin-Releasing Hormone Antagonist. 2. Molecular Dynamics Simulations

Josep Rizo,[†] Steven C. Koerber,[‡] Rachelle J. Bienstock,[†] Jean Rivier,[‡] Lila M. Gierasch,*[,†] and Arnold T. Hagler*[,§]

Contribution from the Department of Pharmacology, University of Texas Southwestern Medical Center, 5323 Harry Hines Boulevard, Dallas, Texas 75235-9041, Biosym Technologies, Inc., 10065 Barnes Canyon Road, San Diego, California 92121, and The Clayton Foundation Laboratories for Peptide Biology, The Salk Institute, 10010 North Torrey Pines Road, La Jolla, California 92037. *Received August 19, 1991*

Abstract: Molecular dynamics simulations in vacuo and in solvent have been used, in combination with the NMR data presented in the preceding paper in this issue, to analyze the conformational behavior of a highly potent antagonist of gonadotropin-releasing hormone (GnRH). An initial conformational search in vacuo yielded two fundamentally different classes of structures that differ in the location of the tail formed by residues 1-3, above or below the cyclic part of the molecule. NMR restraints were applied progressively on both families of structures, leading to a consistent conformational model that confirms and refines the interpretation of the experimental data. The restraints force the orientation of the tail above the ring and induce a β-hairpin structure in residues 5-8, as expected from the NMR analysis. The simulations support the presence of a γ turn around D-Trp3 and indicate the presence of high mobility in residues 1 and 2. Two different conformational equilibria have been characterized in the Asp4-Dpr10 bridge. Frequent contacts between the tail, Tyr5, and Arg8 indicate new bridging constraints to obtain more rigid GnRH antagonists. The biological activity of some bicyclic GnRH analogues that include these constraints supports our refined model for the bioactive conformation of GnRH. Our molecular dynamics results show that only a careful choice of NMR restraints, and their continuous evaluation, can lead to reliable structures when considerable flexibility exists in the molecule. In vacuo, large energy differences are observed between structures with different aromatic side chain rotameric states. We find that conformations that should be visited frequently in our experimental conditions can have energies more than 30 kcal/mol above the lowest energy conformation found in vacuo. These energy differences are mainly due to nonbonding interactions that highly favor compact structures. Simulations carried out in a solvent bath can overcome this problem and yield improved structures, with a lower tendency to form intramolecular hydrogen bonds.

The ability to determine well-defined three-dimensional structures for target compounds is an immensely powerful tool in drug design. A wealth of information on the conformations of small polypeptides in solution, and their sensitivity to the environment, can be obtained by two-dimensional nuclear magnetic resonance (NMR) spectroscopy,[1] and this information can be used in combination with computational techniques such as distance geometry,[2] molecular dynamics,[3] simulated annealing,[4] and variable target function algorithms,[5] to yield the desired three-dimensional structures. Molecular dynamics methods have been recently shown to be extremely powerful in a wide variety of applications to biomolecular problems, including drug design,[6,7] reproduction of structural properties of peptides in solvent environments[8] or in crystals,[9] refinement of protein structures,[10] and studies on protein dynamics[11] and on protein-ligand interactions.[12] Although it can be argued that molecular dynamics simulations are biased by the choice of initial conformations and may search only a limited region of configurational space near these conformations, they most likely constitute the method of choice to obtain energetically reasonable structures[13] and understand the conformational behavior of the molecule under study, in particular when flexibility and conformational equilibria are likely to exist.[3c] In studies of small peptides in solution, a conformational model deduced from NMR data, together with interproton distance, hydrogen bonding, and torsional restraints,[14] can guide the simulations to consistent conformations. The limitations in terms of configurational space searched can be at least partially overcome with high-temperature simulations,[15] dynamic torsional forcing procedures,[7] and a careful analysis of the experimental data in combination with the results of the simulations. A continuous reconsideration of the interpretation of the NMR data, in particular with regard to the possibility of conformational averaging,[16] is essential to obtain realistic structures. The strain energy introduced by the restraints can help to identify these equilibria, but an evaluation of the energy terms that contribute

[†] University of Texas Southwestern Medical Center.
[‡] The Salk Institute.
[§] Biosym Technologies, Inc.

(1) Wüthrich, K. *NMR of Proteins and Nucleic Acids*; John Wiley and Sons: New York, 1986.
(2) (a) Crippen, G. M. *J. Comput. Phys.* **1977**, *26*, 449-452. (b) Havel, T. F.; Kuntz, I. D.; Crippen, G. M. *Bull. Math. Biol.* **1983**, *45*, 665-720.
(3) (a) Karplus, M.; McCammon, J. A. *CRC Crit. Rev. Biochem.* **1981**, *9*, 293-349. (b) van Gunsteren, W. F.; Kaptein, R.; Zuiderweg, E. R. P. In *Nucleic Acid Conformation and Dynamics*; Olson, W. K., Ed.; CECAM: Orsay, 1983; pp 79-92. (c) Hagler, A. T. In *The Peptides: Analysis, Synthesis, Biology*; Udenfriend, S., Meienhofer, J., Hruby, V. J., Eds.; Academic Press: Orlando, FL, 1985; Vol. 7, pp 213-299. (d) Hagler, A. T.; Osguthorpe, D. J.; Dauber-Osguthorpe, P.; Hempel, J. C. *Science* **1985**, *227*, 1309-1315.
(4) Nigles, M.; Clore, G. M.; Gronenborn, A. M. *FEBS Lett.* **1988**, *229*, 129-136.
(5) Braun, W.; Go, N. *J. Mol. Biol.* **1985**, *186*, 611-626.
(6) (a) Struthers, R. S.; Rivier, J.; Hagler, A. T. In *Conformationally Directed Drug Design-Peptides and Nucleic Acids as Templates or Targets*; Vida, J. A., Gorden, M., Eds.; American Chemical Society: Washington, DC, 1984; pp 239-261. (b) Struthers, R. S.; Rivier, J.; Hagler, A. *Ann. N.Y. Acad. Sci.* **1985**, *439*, 81-96.
(7) Struthers, R. S.; Tanaka, G.; Koerber, S.; Solmajer, T.; Baniak, E. L.; Gierasch, L. M.; Vale, W.; Rivier, J.; Hagler, A. T. *Proteins* **1990**, *8*, 295-304.
(8) Lautz, J.; Kessler, H.; van Gunsteren, W. F.; Weber, H. P.; Wenger, R. M. *Biopolymers* **1990**, *29*, 1669-1687.
(9) Kitson, D. H.; Hagler, A. T. *Biochemistry* **1988**, *27*, 5246-5257.
(10) (a) Brunger, A. T.; Kuriyan, J.; Karplus, M. *Science* **1987**, *235*, 458-460. (b) van Gunsteren, W. F. *Stud. Phys. Theor. Chem.* **1990**, *71*, 463-478.
(11) Avbelj, F.; Moult, J.; Kitson, D. H.; James, M. N. G.; Hagler, A. T. *Biochemistry* **1990**, *29*, 8658-8676.
(12) (a) Bash, P. A.; Singh, U. C.; Brown, F. K.; Langridge, R.; Kollman, P. A. *Science* **1987**, *235*, 574-575. (b) Dauber-Osguthorpe, P.; Roberts, V. A.; Osguthorpe, D. J.; Wolf, J.; Genest, M.; Hagler, A. T. *Proteins* **1988**, *4*, 31-47.
(13) See, for instance: Lautz, J.; Kessler, H.; Blaney, J. M.; Scheek, R. M.; van Gunsteren, W. F. *Int. J. Pept. Protein Res.* **1989**, *33*, 281-288.
(14) We use the term *restraint* in the sense indicated by Mackay et al. (Mackay, D. H. J.; Cross, A. J.; Hagler, A. T. In *Prediction of Protein Structure and the Principles of Protein Conformation*; Fasman, G. D., Ed.; Plenum: New York, 1989; pp 317-358), i.e., "a term added to the target function that biases the system toward adopting a certain value for a degree of freedom", reserving the term *constraint* for "degrees of freedom that are fixed".

0002-7863/92/1514-2860$03.00/0

to this strain energy is also necessary to assess the validity of the conformational features that are forced into the molecule. From the point of view of drug design, it is also important to note that molecular dynamics simulations can generate structures of the target compound that, although not observed experimentally, can be accessible to the molecule and related to its bioactive conformation.

In the preceding paper in this issue, we have presented an NMR study of a highly potent gonadotropin-releasing hormone (GnRH) antagonist, Ac-Δ^3-Pro1-D-*p*FPhe2-D-Trp3-c(Asp4-Tyr5-D-2Nal6-Leu7-Arg8-Pro9-Dpr10),[17] which we will refer to as the Asp4–Dpr10 analogue. GnRH is a linear decapeptide, pGlu1-His2-Trp3-Ser4-Tyr5-Gly6-Leu7-Arg8-Pro9-Gly10-NH_2, that plays a key role in mammalian reproduction[18] and, hence, has been the object of intense research efforts to develop analogues that could be used in reproductive therapies or as nonsteroidal contraceptive agents.[19] Design based on the conformational analysis of a marginally potent, cyclic GnRH antagonist (cyclo(Δ^3-Pro1-D-*p*ClPhe2-D-Trp3-Ser4-Tyr5-D-Trp6-NMeLeu7-Arg8-Pro9-β-Ala10)) has led to the development of a series of highly active GnRH antagonists incorporating a bridge between residues 4 and 10;[7] the Asp4–Dpr10 analogue is one of the most potent antagonists in this series. The NMR experiments have allowed us to develop a conformational model for this peptide, with a β-hairpin structure for residues 5–8 in the ring, a relatively more flexible tail (residues 1–3), and a likely conformational equilibrium in the Asp4–Dpr10 bridge. In order to better define these structural features and to have a more accurate understanding of the conformational behavior of the Asp4–Dpr10 analogue, we have carried out a molecular dynamics analysis of this molecule, where particular emphasis has been placed on the selection of restraints and analysis of strain energies that we referred to above. First we conducted a conformational search in vacuo that yielded two main families of conformations differing mainly in the orientation of the tail, above or below the ring. Next, restraints based on the experimental data were introduced in a progressive and "interactive" fashion into the simulations, and closely related structures were obtained starting from either family of conformations. The tail is oriented above the ring in the restrained structures, as was predicted from the NMR data, and frequent interactions between the tail and the Tyr5 and Arg8 side chains were observed, which indicate new bridging opportunities to design more constrained GnRH antagonists. Finally, because structures that should be visited frequently, according to the NMR data, have energies more than 30 kcal/mol above the lowest energy conformation found in vacuo, we included a $CDCl_3$ bath in our simulations to study the effect of the solvent on the calculated conformations. We find that such apparent high strain energies can be justified by differences in solvation energies and, possibly, by entropic effects. Our results emphasize the tendency of calculations carried out in vacuo to favor energetically folded conformations that maximize nonbonding interactions.

Methods

Molecular dynamics simulations and other computational procedures were performed with the DISCOVER and INSIGHTII packages[20] on Silicon Graphics Personal Iris work stations and on CRAY X-MP/48 (San Diego Supercomputer Center, San Diego, CA) or CRAY Y-MP8/864 (Center for High Performance Supercomputing, Austin, TX) supercomputers. A full valence force field[3c] was used to calculate the potential energy. The analytical expression and parameters of this force field have been reported elsewhere.[12b,21] No Morse potentials or cross terms were used in simulations at high temperature. In order to calculate molecular dynamics trajectories, the Newtonian equations of motion were integrated using the Verlet algorithm[22] with a time step of 1 fs. In general, energy minimizations carried out in vacuo consisted of a few steps of steepest descents followed by the conjugate gradient method[23] until the maximum derivative was less than 0.1 kcal/(mol·Å). Vibrational entropies and free energies were calculated using Einstein's equations[24] on structures minimized until the maximum derivative was less than 0.0001 kcal/(mol·Å). Total exposed surface areas were calculated with the Connolly algorithm[25] using a 2.20-Å spherical probe and a 10 points/Å^2 density. Other parameters gave similar areas to those indicated in Table V. The construction of the initial model of the Asp4–Dpr10 analogue is described in the Results and Discussion. All hydrogens were considered explicitly, and no net charge was introduced in the Arg8 residue to maintain the neutrality of the molecule. Interproton distance and hydrogen-bonding restraints were imposed by adding a skewed biharmonic potential[26] to the force field energy. This potential is null between the limits imposed and increases quadratically with the deviation from the bounds outside the null interval to inner and outer extrema where the force becomes constant. During minimizations, the force constants used for intraresidue distances were 15 kcal/(Å^2·mol), except for the Dpr10 NH/NHγ distance; for this interaction, as well as for interresidue distances and hydrogen-bonding restraints, the force constant was 30 kcal/(Å^2·mol). During molecular dynamics simulations, these force constants were multiplied by a factor of $T/300$, where T is the temperature in Kelvin. The maximum force was 100 kcal/(Å·mol) in all calculations. Dihedral angle restraints were harmonic potentials centered on the target value for the corresponding angle. When these restraints were used to keep desired rotameric states, the force constants were 5 kcal/(mol·rad^2), at 300 K, or 15 kcal/(mol·rad^2), at higher temperatures. When used for dynamic torsional forcing procedures,[7] the force constants were 60 or 100 kcal/(mol·rad^2). No torsional restraint was used in any minimization.

Solvent systems were obtained by filling up a 35^3 Å^3 cube with $CDCl_3$ molecules[27] and the Asp4–Dpr10 analogue in the corresponding conformation. Solvent molecules overlapping with the solute were removed, but some percentage of overlapping of the van der Waals radii was allowed to obtain a density of 1.44 g/cm^3. The solvent systems contained 297 $CDCl_3$ molecules, for a total of 1675 atoms including the Asp4–Dpr10 analogue. Periodic boundary conditions were used during the calculations, and charge group-based neighbor lists to calculate nonbonding energies were updated every 20 steps, with a cutoff of 14 Å. A switching function was used to turn off nonbonding interactions, from full strength at 10 Å to 0 at 12 Å. These parameters were considered a good compromise to try to account for most long-range interactions[9] without resulting in excessive computational time (0.34 s of CRAY Y-MP8/864 cpu time per iteration step; 7.5 s in a Silicon Graphics Personal Iris). No intermolecular peptide–peptide interactions exist in these conditions. In order to minimize the initial solvent systems, 100 steps of steepest descents followed by 1000 steps of conjugate gradients[23] were initially used, while allowing only the solvent molecules to move. The resulting systems, and also the instantaneous configurations selected at 5-ps intervals along molecular dynamics trajectories, were minimized, allowing all atoms to move with 100 steps of steepest descents and the conjugate gradient method until the maximum derivative was smaller than 0.5 kcal/(mol·Å). The minimizations took between 8000 and 10 000 steps, and led to average derivatives around 0.02–0.03 kcal/(mol·Å) for the energy of the

(15) diNola, A.; Berensden, H. J. C.; Edholm, O. *Macromolecules* **1984**, *17*, 2044–2050.

(16) (a) Kessler, H.; Griesinger, C.; Lautz, J.; Muller, A.; van Gunsteren, W. F.; Berensden, H. J. C. *J. Am. Chem. Soc.* **1988**, *110*, 3393–3396. (b) Stradley, S. J.; Rizo, J.; Bruch, M. D.; Stroup, A. N.; Gierasch, L. M. *Biopolymers* **1990**, *29*, 263–287.

(17) Nomenclature as indicated in Figure 1 of the preceding paper in this issue.

(18) (a) Vander, A. J.; Sherman, J. H.; Luciano, D. S. *Human Physiology, the Mechanisms of Body Function*; McGraw-Hill: New York, 1970; pp 443–471. (b) Matsuo, H.; Baba, Y.; Nair, R. M. G.; Arimura, A.; Schally, A. V. *Biochem. Biophys. Res. Commun.* **1971**, *43*, 1374–1439. (c) Burgus, R.; Butcher, M.; Amoss, M.; Ling, N.; Monahan, M.; Rivier, J.; Fellows, R.; Blackwell, R.; Vale, W.; Guillemin, R. *Proc. Natl. Acad. Sci. U.S.A.* **1972**, *69*, 278–282.

(19) (a) Vickery, B. H., Nestor, J. J., Jr., Hafez, E. S. E., Eds. *LHRH and Its Analogs: Contraceptives and Therapeutic Applications*; MTP Press: Lancaster, England, 1984. (b) Karten, M.; Rivier, J. *Endocr. Rev.* **1986**, 7, 44–66.

(20) DISCOVER and INSIGHTII are commercially available from Biosym Technologies Inc., 10065 Barnes Canyon Rd, San Diego, CA 92121.

(21) (a) Hagler, A. T.; Lifson, S. *J. Am. Chem. Soc.* **1974**, *96*, 5319–5327. (b) Hagler, A. T.; Dauber, P.; Lifson, S. *J. Am. Chem. Soc.* **1979**, *101*, 5131–5141.

(22) Verlet, L. *Phys. Rev.* **1967**, *159*, 98–103.

(23) Fletcher, R.; Reeves, C. M. *Comput. J.* **1962**, *7*, 149–154.

(24) (a) Hill, T. L. *An Introduction to Statistical Thermodynamics*; Addison-Wesley: Reading, MA, 1960. (b) Hagler, A. T.; Stern, P. S.; Sharon, R.; Becker, J. M.; Naider, F. *J. Am. Chem. Soc.* **1979**, *101*, 6842–6852.

(25) Connolly, M. L. *Science* **1983**, *221*, 709–713.

(26) Vlieg, J.; Boelens, R.; Scheek, R. M.; Kaptein, R.; van Gunsteren, W. F. *Isr. J. Chem.* **1986**, *27*, 181–188.

(27) Parameters to model the $CDCl_3$ molecule were deduced from an ab initio calculation consisting of a Mulliken population analysis and scaling of the charges to fit the experimental dipole moment of chloroform; the atomic partial charges in this model are C, −0.11; Cl, −0.02; H, +0.17. Deuterium was treated as a hydrogen atom with atomic mass 2.

whole system, and to convergence for the energy of the Asp4–Dpr10 analogue molecule (intramolecular plus interactions with the solvent) within ±0.01 kcal/mol.

Results and Discussion

Unrestrained Dynamics in Vacuo. Conformational Search. The design of the Asp4–Dpr10 GnRH analogue was based on a putative binding conformation proposed for the cyclic GnRH antagonist cyclo(Δ^3-Pro1-D-*p*ClPhe2-D-Trp3-Ser4-Tyr5-D-Trp6-NMeLeu7-Arg8-Pro9-β-Ala10).[6,7] Accordingly, we generated an initial structure for the Asp4–Dpr10 analogue from the minimum energy conformation found for the parent cyclic decapeptide antagonist. Lacking parameters to model D-*p*FPhe2, we constructed our model for the Asp4–Dpr10 analogue with a D-Phe2 residue.[28] The appropriate residues in the cyclic decapeptide structure were mutated (maintaining the corresponding torsion angles where possible), interactive manipulation was used to close the Asp4–Dpr10 bridge and to remove severe side chain overlap, and an initial minimization was conducted while tethering the backbone atoms. Further minimization without the tethering potential yielded the initial conformation of the Asp4–Dpr10 analogue with an energy of 188.5 kcal/mol. In order to search conformational space, a 50-ps, 900 K simulation was then carried out, and the minimum energy conformation found along the trajectory (176.6 kcal/mol) was subsequently annealed at 300 K for two periods of 50 ps. The lowest energy conformation found in the first annealing trajectory (174.0 kcal/mol) was used as initial structure for the second trajectory, where no lower energy conformations were found. The structures visited during all these simulations belong essentially to the same conformational family, and they are characterized by the location of the tail above the ring. The minimum energy conformation in this family, which we will refer to as TU (tail-up), is represented in Figure 1.

In order to explore further the conformational space available to the Asp4–Dpr10 analogue, we employed a dynamic torsional forcing algorithm[7] where the backbone ϕ and ψ angles were sequentially forced to rotate through 180° over a period of 1 ps, for a total trajectory of 18 ps (Δ^3-Pro1 and Pro9 ϕ were not forced). A major event occurred in the central part of the trajectory: the tail formed by residues 1–3 moved below the ring and remained on this side for the rest of the trajectory. The lowest energy conformation with this tail orientation had an energy of 202.4 kcal/mol, but a succession of 900 K simulations, annealing trajectories at 300 K, and energy minimizations yielded an energy minimum of 171.3 kcal/mol. The structure obtained is very similar to the minimum energy conformation previously reported for the analogous cyclo(4–10) GnRH antagonist incorporating a Dpr4–Asp10 bridge (instead of Asp4–Dpr10),[29] with a different orientation for the Trp3 and 2Nal6 side chains. Indeed, when the same orientation for these side chains was introduced in the Asp4–Dpr10 analogue, and an annealing trajectory of 50 ps at 300 K was calculated, a conformation of 166.5 kcal/mol was obtained. This structure, which we will refer to as the TD (tail-down) conformation, is the lowest energy conformation found to date, in vacuo, for the Asp4–Dpr10 analogue (Figure 1).

Restrained Molecular Dynamics in Vacuo. The conformational behavior of a molecule is necessarily dependent on the environment unless it is extremely rigid.[9,30] An ensemble of conformations is to be expected in solution, and the various conformations will differ to a greater or lesser extent as a function of the flexibility of the molecule. The nonbonding interactions with the solvent will influence the conformational distribution, and hence, it is hardly reasonable to expect to reproduce this distribution with molecular dynamics simulations in vacuo unless the calculations are biased with restraints deduced from the experimental data. However, we mentioned earlier that a careful choice of the restraints is critical, as the experimental measurements can correspond to averaged values that may not be compatible with single real conformations. In keeping with this reasoning, we introduced NMR restraints in the calculated conformations of the Asp4–Dpr10 analogue in a progressive fashion, analyzing the effect of the restraints in each step.

The conclusions drawn from the NMR data obtained in $CDCl_3$/DMSO-d_6 (5:1) (see preceeding paper in this issue) can be summarized as follows: (i) residues 5–8 adopt a β-hairpin structure, which includes a type II′ β turn around residues 6 and 7 and two transannular hydrogen bonds (Tyr5 NH/Arg8 CO and Arg8 NH/Tyr5 CO); (ii) there is clear evidence for a conformational equilibrium in the Asp4–Dpr10 bridge, with Dpr10 NHγ being somewhat sequestered from the solvent; (iii) the tail (residues 1–3) is oriented above the ring; (iv) a γ turn around D-Trp3, closed by a hydrogen bond between the Asp4 NH and the D-Phe2 CO, is likely to exist, while residues 1 and 2 appear to be flexible and could be visiting frequently a type II β-turn conformation; (v) the $\chi_1 = 60°$ side chain rotamer is preferred in D-Phe2 and D-Trp3, and possibly, in D-2Nal6. Taking into account these conformational characteristics, only 19 interproton distances were proposed to be used as restraints, at least in a first approach[31] (see preceding paper in this issue, Table IV). Although some of these restraints still correspond to regions of the molecule that were suspected to have some flexibility, they can be introduced to test their compatibility with single conformations. We started our restrained molecular dynamics study by restraining the 19 interproton distances, and additional restraints were used in later stages of the analysis to force hydrogen bonds and side chain torsion angles. The restraints used to obtain the structures described below are indicated in Table I. Other parameters that were not restrained were also constantly monitored to assess the quality of our model, in particular the transannular Asp4 Hα/Pro9 Hα, Asp4 Hα/Dpr10 NH, and Tyr5 NH/Arg8 NH distances (weak NOEs are observed between the corresponding protons).

Interproton Distance and Transannular Hydrogen Bond Restraints. The conformational search described above yielded two main structural families which differ primarily in the orientation of the tail with respect to the ring. Conformational parameters characterizing the TU and TD conformations (total deviation of the interproton distances with respect to the limits estimated from the NMR data, the three transannular distances mentioned above, hydrogen bonding patterns, and selected torsion angles) are given in Tables I–III. As could be expected from the analysis of the NMR data, the measured interproton distances agree significantly better with the TU than with the TD conformation (Table I). The transition from the TU to the TD conformation is produced by a radical change in Asp4 ψ, which has a negative value in TD (Table II). In Figure 2 it can be observed how this transition brings Asp4 Hα, which is pointing inside the ring in TU, to be oriented outside the ring in TD, distant from Tyr5 NH, Pro9 Hα, and Dpr10 NH. Note that this arrangement is inconsistent with the NOEs observed between Asp4 Hα and these three protons.

The 19 interproton distance restraints were easily accomodated into the TU conformation. A 50-ps, 900 K molecular dynamics simulation with these restraints gave a 179.4 kcal/mol minimum energy structure that fits perfectly all the distances within the experimental limits. The force constant used on all the restraints to minimize this structure was 30 kcal/(Å^2·mol). When the force constant for the intraresidue restraints (except for that on Dpr10 NH/NHγ) is decreased to 15 kcal/(Å^2·mol) in the minimization,

(28) The presence of a halogen atom (F or Cl) in position 4 of the aromatic ring of D-Phe2 appears to be important for the biological activity of GnRH antagonists. However, this observation could be related to a direct interaction of the halogen atom with the GnRH receptor, and it is unlikely that this modification has a substantial effect on the conformation of the Asp4–Dpr10 analogue. The last assumption is supported by the NMR data, which indicates high mobility for the D-*p*FPhe2 aromatic ring, and also by the structures obtained in the molecular dynamics simulations described below.

(29) Rivier, J.; Koerber, S.; Rivier, C.; Hagler, A.; Perrin, M.; Gierasch, L.; Corrigan, A.; Porter, J.; Vale, W. In *International Symposium on Frontiers in Reproduction Research: The Role of Growth Factors, Oncogenes, Receptors and Gonadal Polypeptides*, Beijing, China; Chen, H.-C., Ed.; in press.

(30) Fisher, C. L.; Roberts, V. A.; Hagler, A. T. *Biochemistry* **1991**, *30*, 3518–3526.

(31) Unless otherwise noted, only these 19 interproton distances will be considered when accounting for deviations between experimental and calculated distances.

Table I. Characterization of Selected Conformations of the Asp4–Dpr10 Analogue: Restraints Used To Obtain Them, Energies, Total Distance Violations, and Transannular Interproton Distances[a]

	TD	TDC1	TDC2U	TDC3U	TDC4U	TU	TUC1	TUC2	TUC3	TUC4	TUC5	TUC6	TUC7	TUC6S[i]
restraints[b]														
interproton dist[c]		19	19	19	19		19	19	19	19	19	19	19	19
hydrogen bonds[d]			AB	ABCD	EBCD			AB	ABCD	ABCD	ABC	EBCD	EBC	EBCD
side chains[e]					FWYNa					FW	FW	FWNa	FWNa	
energy (kcal/mol)	166.5	185.0	188.4	186.0	201.2	174.0	176.3	182.9	181.7	190.7	189.8	199.5	198.2	207.2
Δ(dist)[f] (Å)	3.42[g]	0.34	0.39	0.39	0.50	1.97[h]	0.54	0.57	0.41	0.42	0.41	0.47	0.43	0.44
D4 Hα/P9 Hα (Å)	6.53	6.42	2.79	3.52	3.19	4.19	4.32	4.02	3.66	3.61	3.74	3.52	3.98	4.06
D4 Hα/Dp10 NH (Å)	5.33	5.40	2.98	3.19	3.06	4.02	3.68	3.27	3.31	3.34	3.76	3.31	3.96	3.68
Y5 NH/R8 NH (Å)	3.91	5.58	3.76	3.62	3.46	3.34	3.31	3.26	3.48	3.35	3.65	3.33	3.64	3.33

[a] The mnemonic code used to name the structures is based on the orientation of the tail (T) with respect to the ring, up (U) or down (D); C indicates restrained, and U has been added to the name of some of the restrained structures obtained from TD to reflect the fact that the tail moved up as a result of the restraints. Further details on how these structures were obtained can be found in the text. [b] Note that some of the restraints used in the molecular dynamics simulations leading to these structures are different from those used in the minimizations. The force constants for interproton distance and hydrogen bond restraints during the simulations were those indicated for the minimizations multiplied by a factor of $T/300$, where T is the temperature in Kelvin. No side chain torsion was restrained in any minimization. [c] The number 19 indicates that the 19 interproton distances indicated in Table IV of the preceding paper in this issue were restrained; the force constants used in the minimizations leading to these structures were 30 kcal/(Å^2·mol) for interresidue distances and Dpr10 NH/NHγ and 15 kcal/(Å^2·mol) for all other intraresidue distances. [d] Hydrogen bonds were restrained with a force constant of 30 kcal/(Å^2·mol) during minimizations. The limits of the restraint were 1.9–2.4 Å for Arg8 N*H*/Tyr5 C*O* (A), Tyr5 N*H*/Arg8 C*O* (B), Asp4 N*H*/D-Phe2 C*O* (C), and Dpr10 N*H*γ/D-Trp3 C*O* (D); Arg8 N*H*/Tyr5 C*O* was restrained to 1.9–2.1 Å in some of the simulations (E). [e] Side chain χ_1 torsion angles forced during the simulations leading to the corresponding structures. The symbols F, W, Y, and Na indicate that the D-Phe2, D-Trp3, Tyr5, or D-2Na16 side chains, respectively, were forced to adopt the rotamer with χ_1 = 60°. The aromatic side chain χ_1 torsion angles for some of these structures are indicated in Table II. The torsional restraints were removed during the minimizations (see text and Methods for further details). [f] Total deviation with respect to the limits given for the 19 interproton distances indicated with an asterisk in Table IV of the preceding paper. [g] Largest deviation: Asp4 Hα/Tyr5 NH, 0.90 Å above the upper bound. [h] Largest deviation: Dpr10 NH/NHγ, 0.75 Å above the upper bound. [i] Minimum energy structure found in a restrained molecular dynamics simulation carried out with solvent (see text and Table V). All aromatic side chains were in the χ_1 = 60° rotameric state in the starting conformation, and they were not forced during the simulation. The energy refers to intramolecular energy in the Asp4–Dpr10 analogue molecule.

Table II. Selected Dihedral Angles in Different Conformations of the Asp4–Dpr10 Analogue

torsion angle	TD	TDC2U	TDC3U	TDC4U	TU	TUC2	TUC3	TUC4	TUC5	TUC6	TUC7	TUC6S
Δ^3-Prol φ	−76	−71	−71	−61	−74	−73	−77	−76	−79	−75	−79	−71
Δ^3-Prol ψ	88	86	86	128	88	87	89	169	67	162	67	158
D-Phe2 φ	69	123	101	128	106	125	112	149	115	134	114	140
D-Phe2 ψ	51	−54	−32	−60	−76	−76	−62	−77	−80	−70	−79	−73
D-Trp3 φ	83	93	89	101	124	143	95	98	67	97	69	90
D-Trp3 ψ	−90	−93	−82	−63	−119	−96	−76	−76	−101	−76	−101	−70
Asp4 φ	−101	−130	−115	−125	−109	−132	−115	−128	−96	−130	−95	−122
Asp4 ψ	−60	69	81	91	96	92	94	93	83	102	84	99
Tyr5 φ	−153	−166	−121	−154	−147	−156	−148	−150	−145	−150	−146	−157
Tyr5 ψ	104	141	51	89	36	61	65	60	57	92	76	100
D-2Na16 φ	92	76	60	70	84	69	60	68	67	71	71	65
D-2Na16 ψ	−88	−109	−82	−94	−68	−81	−81	−81	−79	−95	−89	−109
Leu7 φ	−124	−81	−58	−68	−61	−57	−54	−57	−56	−68	−62	−71
Leu7 ψ	66	−26	−31	−21	−48	−29	−35	−27	−32	−24	−30	−7
Arg8 φ	−146	−121	−95	−112	−96	−98	−100	−104	−103	−98	−97	−92
Arg8 ψ	85	107	−105	97	107	99	105	103	116	111	117	113
Pro9 φ	−74	−65	−88	−67	−86	−87	−87	−87	−82	−87	−81	−85
Pro9 ψ	108	160	149	152	144	128	140	142	159	147	156	139
Dpr 10 φ	−86	−81	−85	−80	−88	−80	−84	−85	−83	−80	−84	−90
Asp4 χ_1	−64	−101	−92	−93	−155	−123	−88	−91	−68	−91	−67	−81
Asp4 χ_2	100	77	37	67	109	68	24	36	−77	65	−78	29
Dpr10 χ_1	−59	−64	−58	−63	−69	−62	−56	−62	−61	−64	−64	−65
Dpr10 χ_2	177	94	129	95	109	128	135	136	−93	94	−92	145
D-Phe2 χ_1	180	78	67	78	161	159	158	73	79	77	77	72
D-Trp3 χ_1	163	166	174	56	177	179	174	59	79	57	79	77
Tyr5 χ_1	−170	180	−172	73	69	55	61	52	56	71	55	53
D-2Na16 χ_1	67	158	−55	68	−65	−63	−64	−63	−58	67	65	67

the energy decreases to 176.3 kcal/mol (only 2.3 kcal/mol above the unrestrained TU conformation), while only one distance (Trp3 NH/Hα) deviates more than 0.1 Å from the experimental bounds. On the basis of these observations, we decided to keep the 19 interproton distance restraints and to use the weaker force constants for intraresidue restraints in the successive simulations (see Table I and Methods). We will refer to the 176.3 kcal/mol conformation as TUC1 (Table I). This structure is very similar to TU (0.07-Å root mean square (rms) deviation for backbone atoms), which underlines how well the interproton distance restraints are accomodated in the tail-up structures. The TUC1 conformation was used to start a 20-ps, 500 K simulation where two additional restraints were included to force the transannular hydrogen bonds Tyr5 NH/Arg8 CO and Arg8 NH/Tyr5 CO (note that the first one was already present in TU, Table III). This simulation yielded a minimum energy conformation of 182.9 kcal/mol (TUC2, Tables I–III). Although the strain energy introduced was relatively high, these restraints affect several degrees of freedom in the molecule and the NMR data supporting the type II′ β-turn conformation around residues 6 and 7 are quite conclusive. Indeed, lower energy conformations including these restraints were obtained in ensuing simulations, and at least part of the strain energy is due to the lack of solvent in the calculations (see below).

We also tested the effect of the 19 interproton distance restraints on the TD conformation. Not surprisingly, the tail moved from below to above the ring during a 50-ps, 900 K molecular dynamics simulation incorporating these restraints (Figure 3a). The lowest energy conformation where the tail is still below the ring (TDC1, Table I) has a 18.5 kcal/mol strain energy over TD. As a result

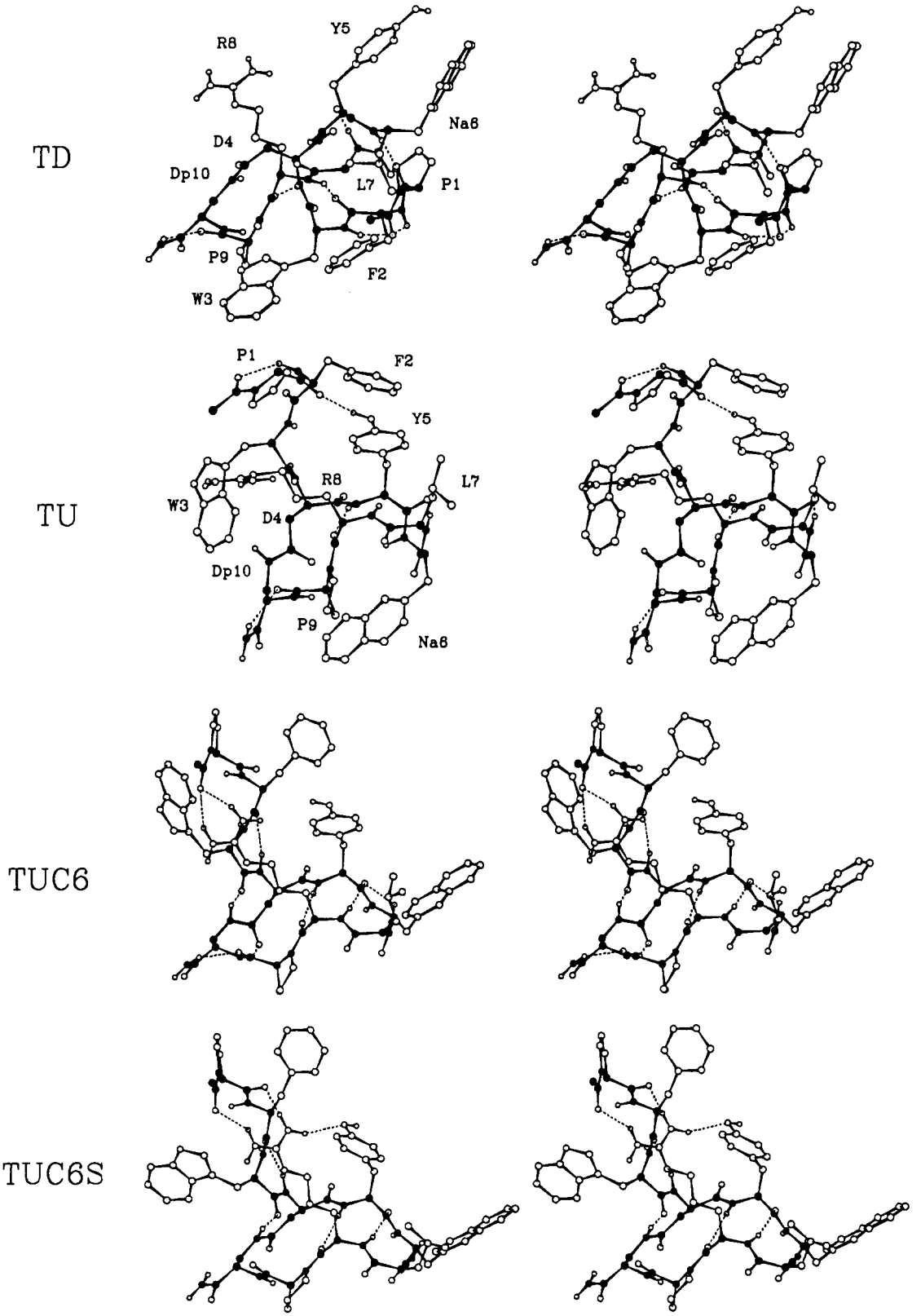

Figure 1. Stereo pairs corresponding to selected structures obtained in the molecular dynamics analysis of the Asp4–Dpr10 analogue (see text). Conformational parameters for these structures are given in Tables I–III. Only hydrogens bonded to heteroatoms have been included. Solid circles correspond to N and C atoms in the backbone and in the side chains forming the bridge (Asp4 and Dpr10). Hydrogen bonds are indicated by dashed lines.

of the restraint on Asp4 Hα/Tyr5 NH, a rotation around Asp4 ψ occurred to reach a value of 90° in this structure, but the rotation brought Tyr5 NH outside the ring rather than bringing Asp4 Hα inside. Note that the Tyr5 NH needs to be oriented inside the ring to explain the observed Tyr5 NH/Arg8 NH NOE and to form a transannular hydrogen bond with Arg8 CO. In accordance with these observations, the tail moved very quickly (a few picoseconds) from below to above the ring when TDC1 was used to start a 50-ps, 900 K simulation where the transannular hydrogen bonds were forced, in addition to the interproton distances (Figure 3b). These results ratify our previous assessment that only tail-up conformations are consistent with the NMR data. Because of

Table III. Hydrogen Bonds in Different Conformations of the Asp4–Dpr10 Analogue[a]

	TD	TDC2U	TDC3U	TDC4U	TU	TUC2	TUC3	TUC4	TUC5	TUC6	TUC7	TUC6S
D-Trp3 NH/Ac CO	x			x								
Asp4 NH/Arg8 CO	x											
D-2Na16 NH/Δ^3-Prol CO	x											
Arg8 NH/D-Phe2 CO	x											
Tyr5 NH/D-Trp3 CO									x		x	
Dpr10 NH/Asp4 COδ		x		x						x		
Arg8 NHη12/Pro9 CO						x						
Arg8 NHη22/Pro9 CO			x	x								
D-Phe2 NH/Ac CO	x	x	x		x	x	x		x		x	
Leu7 NH/Tyr5 CO	x		x	x	x	x	x	x	x	x	x	
NH_2 H2/Pro9 CO	x	x	x	x	x	x	x	x	x	x	x	
Tyr5 NH/Arg8 CO		x	x	x	x	x	x	x	x	x	x	x
Arg8NH/Tyr5 CO		x	x	x		x	x	x	x	x	x	x
Asp4 NH/D-Phe2 CO			x	x			x	x	x	x	x	x
Dpr10 NHγ/D-Trp3 CO		x	x	x			x	x		x		x
Arg8 NHη11/D-Trp3 CO						x						
Arg8 NHη12/Δ^3-Prol CO								x	x		x	x
Arg8 NHη21/Ac CO								x		x		x
Arg8 NHη12/Ac CO										x		
Arg8 NHη11/Tyr Oη								x	x		x	x
Tyr5 OHη/Δ^3-Prol CO				x	x		x					

[a] A proton and an acceptor atom are considered hydrogen bonded when the distance between them is less than 2.5 Å. The hydrogen bonds in italics are the ones proposed to exist according to the analysis of the NMR data and the results of the molecular dynamics simulations.

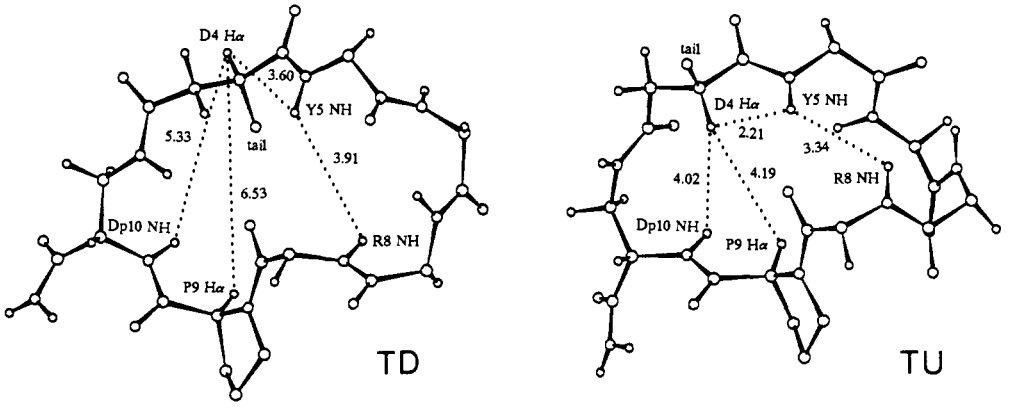

Figure 2. Conformation of the ring (residues 4–10) in the TD and TU structures. Residues 1–3 and side chains of residues 5–8 have been omitted. The critical interproton distances that define the orientation of the tail with respect to the ring are indicated. Only the tail-up conformations can explain the experimental observations: weak Asp4 Hα/Pro9 Hα, Asp4 Hα/Dpr10 NH, and Tyr5 NH/Arg8 NH NOEs are observed by NMR, and the Asp4 Hα/Tyr5 NH distance measured is 2.5 Å (see preceding paper in this issue).

the slow time scale of the NMR measurements, the possibility that a small population of tail-down conformations exists in our experimental conditions, in equilibrium with the predominant tail-up structures, cannot be discarded. However, the fact that the experimental distances are easily fit into the tail-up structures indicates that if any population of tail-down conformations exists, it is sufficiently low so that it can be ignored in our conformational analysis. We continued the refinement of our model for the Asp4–Dpr10 analogue with the restrained structure obtained from the TU conformation (TUC2). The minimum energy structure with the tail up obtained by restraining the TD conformation (TDC2U, Tables I–III) was also refined with similar restraints to test the consistency of our results (see below).

Restraints To Force Side Chain Rotamers and Additional Hydrogen Bonds. The rotameric states of the D-Phe2 and D-Trp3 side chains in TUC2 are essentially the same as in the unrestrained TU structure (Table II) and do not correspond to the preferred ones according to the NMR data (χ_1 = 60° in both cases). Hence, we carried out a 600 K molecular dynamics trajectory where the D-Phe2 and D-Trp3 χ_1 dihedral angles were sequentially forced to decrease from their values in the TUC2 conformation to 60° in 10° steps (0.5 ps/step); after the torsional forcing procedure, the simulation was continued for 20 ps without dihedral angle restraints. Both side chains returned quickly to the original rotameric states when the torsional restraints were relieved, but interesting features were observed in many of the structures obtained: hydrogen bonds between Asp4 NH and D-Phe2 CO and

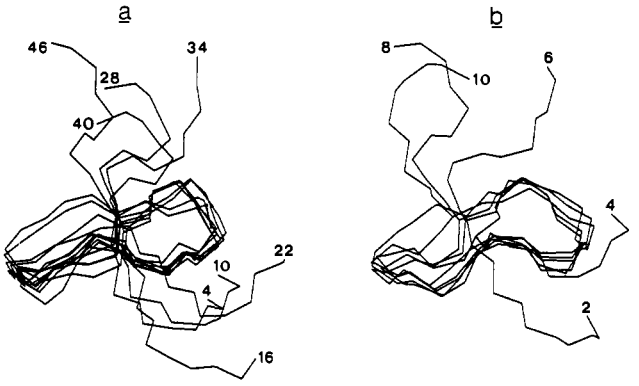

Figure 3. Effect of the interproton distance and transannular hydrogen bond restraints on the TD conformation. The backbone atoms of residues 4–10 in a series of minimized structures, taken along two restrained molecular dynamics simulations started with tail-down conformations, have been superimposed to compare the location of the tail with respect to the ring in the different structures. The N-termini have been labeled with numbers that indicate the time corresponding to each structure in the trajectories (a) 50-ps, 900 K simulation with interproton distance restraints started from TD; the tail moves above the ring in the middle of the trajectory. (b) 50-ps, 900 K simulation with interproton distance and transannular hydrogen bond restraints started from the minimum energy tail-down conformation obtained in (a) (only structures visited in the first 10 ps are shown); the tail moved above the ring in the initial 10 ps and stayed with this orientation for the rest of the trajectory.

between Dpr10 NHγ and D-Trp3 CO had been formed spontaneously. The first of these hydrogen bonds had been proposed from the NMR data, and its presence in the simulations without a direct restraint forcing it gives support to the proposal. The Dpr10 NHγ/D-Trp3 CO hydrogen bond is also present in the structure obtained by restraining the TD conformation, TDC2U (Table III), and could explain the relatively low temperature coefficient of Dpr10 NHγ. Computer graphics shows that D-Trp3 CO comes in close proximity to the Asp4–Dpr10 bridge, as a result of the restraints, and favorable electrostatic interactions with Dpr10 NHγ are therefore established for proper orientations of the central amide bond in the bridge. To explore further the likelihood of these two interactions, first we conducted a minimization of TU where restraints forcing these two hydrogen bonds were added to the interproton distance and transannular hydrogen bond restraints. Indeed, the conformation obtained (TUC3, Tables I–III) has lower energy than TUC2, showing that this conformation was not completely relaxed and that the new restraints do not induce additional strain energy onto the molecule. On the other hand, we wanted to anneal the structure obtained after torsionally forcing D-Phe2 and D-Trp3 χ_1 to 60° and test the stability of the Dpr10 NHγ/D-Trp3 hydrogen bond without a direct restraint to force it. A 40-ps, 300 K simulation was conducted where only an Asp4 NH/D-Phe2 CO restraint was added to the interproton distance and transannular hydrogen bond restraints (no torsional restraints included). Several observations in this simulation are worth noting: (i) the D-Phe2 and D-Trp3 side chains remained around the $\chi_1 = 60°$ rotameric state at this temperature; (ii) the Asp4 NH/D-Phe2 CO distance remained within the limits imposed in most of the minimized structures obtained, confirming the stability of this hydrogen bond; (iii) interestingly, a conformational equilibrium occurs around the Asp4–Dpr10 bridge. We will discuss this equilibrium later, but for the moment, we should point out that two families of structures with different bridge conformation were visted along the simulation, and that the Dpr10 NHγ/D-Trp3 CO hydrogen bond was present in most of the structures from one family and completely absent in the other family. We will refer to the minimum energy conformations corresponding to each family, found along the trajectory, as TUC4 and TUC5 (Tables I–III). In the next simulations we maintained the restraint on Asp4 NH/D-Phe2 CO; the Dpr10 NHγ/D-Trp3 CO hydrogen bond was only forced on the first family of conformations in the ensuing calculations. We will analyze later the high strain energy introduced when the aromatic side chains are forced to adopt the preferred rotameric states.

Although the restraints imposed so far define a type II′ β turn around residues 6 and 7, the torsion angles of these residues in the structures obtained (Table II) are somewhat far from an ideal β turn,[32] and the Arg8 N*H*/Tyr5 C*O* distance is always longer than 2.4 Å (the upper bound of the restraint imposed). The deformation in the turn is most likely due to the Leu7 NH/Tyr5 CO interaction observed in most calculated structures (Table III) (see below). To try to force the molecule to take up a conformation closer to a type II′ β turn, we decreased the upper bound of the restraint to 2.1 Å in some of our next calculations. On the other hand, another factor that could be deforming the structure of the turn to some extent is the D-2Nal6 side chain, which is located below the ring, interacting strongly with the atoms located on this side of the molecule, and occupying the $\chi_1 = -60°$ rotameric state (Table II). When the rotameric state with $\chi_1 = 60°$, which is likely to be preferred according to the NMR data, is imposed interactively on structures TUC4 and TUC5, it can be observed that the D-2Nal6 side chain points outside the molecule and no steric conflicts occur. We carried out a 20-ps, 300 K simulation, starting with a structure analogous to TUC4, with D-2Nal6 $\chi_1 = 60°$, and setting the upper bound of the Arg8 NH/Tyr5 CO restraint to 2.1 Å. A 199.5 kcal/mol minimum energy structure resulted from this simulation (TUC6, Tables I–III, Figure 1). If the minimizations are carried out with the usual upper limit for the Arg8 NH/Tyr5 CO restraint, 2.4 Å, the minimum obtained has an energy of 199.3 kcal/mol. Hence, the tighter restraint on the hydrogen bond does not induce high strain in the molecule, while the torsion angles of residues 6 and 7 in the structure obtained were somewhat closer to an ideal type II′ β turn (Table II). A structure analogous to TUC5, with D-2Nal6 $\chi_1 = 60°$, was also minimized with the tighter restraint in the hydrogen bond closing the β turn, resulting in structure TUC7 (Tables I–III). Note the high increase in energy that also results when this aromatic side chain is moved from the original position in the unrestrained TU structure, as occurred with the D-Phe2 and D-Trp3 side chains.

Consistency of the Conformational Model. The molecular dynamics simulations described above have led to a refinement of our conformational model for the Asp4–Dpr10 analogue, yielding structures (TUC6, TUC7) that should be closely related to those preferentially sampled in the experimental conditions. Structures that differ from TUC6 and TUC7 primarily in the aromatic side chain rotamers (e.g., TUC3–TUC5) should also be significantly populated, as none of the rotamers is 100% populated. In Table I we can observe that the total deviation of the interproton distances in the restrained structures (TUC1–TUC7), with respect to the experimental limits, did not increase significantly when other restraints were introduced in the molecule. Morever, in very few cases are the individual deviations higher than 0.1 Å, and only the D-Phe2 NH/D-Trp3 NH and Dpr10 NH/NHγ distances deviate more than 0.2 Å, in some cases, when the structures are further minimized without any restraints. These observations confirm that the experimental interproton distances are, in general, well accommodated in the conformational model that has emerged from the calculations. Further confirmation for this model is afforded by the transannular Tyr5 NH/Arg8 NH, Asp4 Hα/Dpr10 NH, and Asp4 Hα/Pro9 Hα distances (Table I). The first two are short enough in all these structures to justify the observation of NOE interactions, while the Asp4 Hα/Pro9 Hα distance decreased gradually as the NMR restraints were included. Indeed, monitoring this last distance along the molecular dynamics trajectories shows that it experiences large oscillations with the molecular motions (in general between 3.0 and 4.5 Å), and sometimes is as short as 2.5 Å. The simulations give support to the existence of a hydrogen bond between Asp4 NH and D-Phe2 CO and suggest that Dpr10 NHγ is hydrogen bonded to D-Trp3 CO in some of the preferred conformations. Although the hydrogen-bonding patterns have evolved to a better agreement with the NMR data, as a consequence of the restraints, an excessive number of hydrogen bonds is observed in the calculated structures (Table III), which may well be attributed to the lack of solvent in the calculations (see below).

An important question that remains to be answered about our conformational model is whether there are other conformations, substantially different from the restrained structures obtained so far, that can also fit the NMR observations. We also want to consider two other aspects of the conformational behavior of the Asp4–Dpr10 analogue that are related to this question: the flexibility of the tail and the conformational equilibrium in the Asp4–Dpr10 bridge.

Structures Obtained Starting from the Tail-Down Structure. The TD conformation represents a very different fold of the Asp4–Dpr10 analogue, compared to the tail-up structures: the rms deviation for the backbone atoms between TD and TUC3–TUC7 ranges from 3.7 to 4.1 Å. Hence, one test for the consistency of our model is the comparison of TUC3–TUC7 with conformations obtained by restraining TD. We described above that forcing the interproton distance and transannular hydrogen bond restraints on TD led to tail-up structures such as TDC2U. A 50-ps, 600 K simulation was started with this conformation adding the Asp4 NH/D-Phe2 CO and Dpr10 NH/D-Trp 3 CO restraints. A 186.0 kcal/mol minimum energy conformation was obtained (TDC3U, Tables I–III), and after torsionally forcing the same rotameric states for the aromatic side chains present in TUC6 and TUC7, another 50-ps, 600 K trajectory was calculated. The last simu-

(32) Rose, G. D.; Gierasch, L. M.; Smith, J. A. *Adv. Protein Chem.* **1985**, *37*, 1–109.

Table IV. Root Mean Square Deviations (Å) for Backbone Atoms (above Diagonal) and for Backbone Atoms of Residues 3–10 (below Diagonal) between Selected Structures of the Asp4–Dpr10 Analogue

	TDC3U	TDC4U	TUC3	TUC4	TUC5	TUC6	TUC7
TDC3U		0.77	0.79	1.46	1.64	1.27	1.66
TDC4U	0.58		0.60	1.18	1.44	0.78	1.42
TUC3	0.27	0.51		0.80	1.07	0.71	1.09
TUC4	0.34	0.56	0.20		0.70	0.70	0.74
TUC5	0.46	0.55	0.37	0.28		1.06	0.23
TUC6	0.62	0.27	0.56	0.61	0.60		1.00
TUC7	0.51	0.47	0.45	0.39	0.24	0.45	

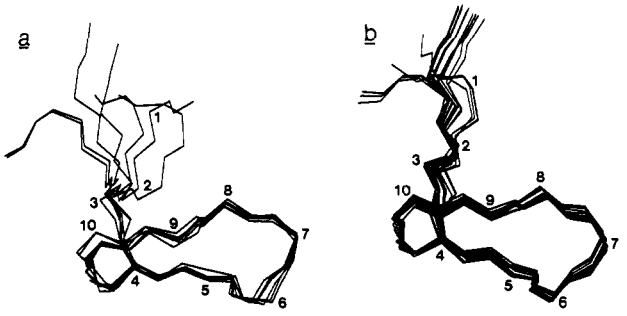

Figure 4. Superposition of the backbone of (a) selected conformations of the Asp4–Dpr10 analogue obtained with our restrained molecular dynamics analysis (structures TDC3U, TDC4U, and TUC3–7, Tables I–III) and (b) 20 minimized structures obtained at 2-ps intervals along the 40-ps, 300 K molecular dynamics simulation that led to structures TUC4 and TUC5 (see text). The numbers indicate the positions of the Cα carbons. Note the flexibility of the tail, increasing from the end attached to the ring to the N-terminus (what we could call a whip effect). Note that more that one conformation is also visited in the Asp4–Dpr10 bridge.

lation resulted in a minimum energy conformation of 201.2 kcal/mol (TDC4U, Tables I–III). The backbone rms deviations for TUC3–TUC7 and TDC3U–TDC4U are shown in Table IV, where they are compared with rms deviations for the backbone atoms of residues 3–10 in the same structures. A superimposition of the backbone atoms of all these conformations is shown in Figure 4a. We can observe that there is a variable degree of similarity among these structures, but the largest deviations are due to different conformations in residues 1 and 2. When these residues are not taken into account, the largest rms deviation between any of the structures is 0.62 Å, and deviations as low as 0.27 Å are observed between structures obtained by restraining TD and structures obtained from TU (TDC3U/TUC3 and TDC4U/TUC6, Table IV). These results give support to the coherence of the overall fold of the structures obtained.

Flexibility of the Tail. The NMR data described in the preceding paper in this issue indicate that some flexibility is likely to exist in the tail (residues 1–3) of the Asp4–Dpr10 analogue, in particular in residues 1 and 2. The rms deviations described above and the variability of the torsion angles of residues 1 and 2 in the calculated structures (Table II) indicate that several conformations of these residues were visted during the simulations, despite the use of several restraints in this region of the molecule. The torsion angles (Table II) also indicate some degree of flexibility in D-Trp3, notwithstanding the fact that this residue is in the corner position of a γ turn. The superposition of minimized structures taken along one of the trajectories calculated at 300 K (Figure 4b) shows that several conformations of the tail are visited in the time scale of the simulation (40 ps) even at this temperature. Most of the restraints in residues 1 and 2 are well accepted in the minimized structures, and almost identical conformations are obtained in some cases when the minimizations are carried out without these restraints. The D-Phe2 NH/D-Trp3 NH distance has a tendency to be longer than the experimental upper limit (3.1 Å) in many structures and can take values between 3.2 and 3.7 Å when minimized without restraints. However, this distance is well within the experimental limits in structures such as TDC4U that include a conformation similar to a type II β turn around residues 1 and 2, closed by a hydrogen bond between D-Trp3 NH and Ac CO (Table III). All these observations indicate that there is high flexibility in residues 1 and 2 and support the proposal from the NMR analysis that conformations similar to a type II β turn around these residues are visited frequently. The interproton distances measured in this region of the molecule should correspond to averages over the ensemble of conformations that are actually being populated under the experimental conditions, and the conformations of residues 1 and 2 in the calculated structures represent, at most, part of this ensemble. Finally, it should also be noted that the γ turn around D-Trp3 that appears to be present in $CDCl_3$/DMSO-d_6 (5:1 (v/v)) is disrupted in DMSO-d_6 (see preceding paper in this issue), which underlines the flexibility of the linear part of the Asp4–Dpr10 analogue.

Conformational Equilibrium in the Asp4–Dpr10 Bridge. In the preceding paper in this issue, we indicate that some of the NMR interproton distances involving the Asp4 and Dpr10 side chains cannot correspond to a single conformation of the Asp4–Dpr10 bridge and that the broadening of the signals corresponding to protons in this region of the molecule suggests a relatively slow conformational equilibrium within the bridge. On the other hand, it has been pointed out above that two structural families with different bridge conformation were observed along the dynamics trajectory that yielded structures TUC4 and TUC5. In Figure 5 is shown the evolution of the Asp4 and Dpr10 χ_2 dihedral angles along this trajectory, where the rapid interconversion between these conformational families that occurs on the time scale of the simulation is illustrated. As was predicted, this interconversion implies a rotation around the amide bond in the center of the bridge, and analysis of the interproton distances within the bridge in structures TUC4–TUC7 (data not shown) indicates that most of the experimental distances can be explained by an equilibrium between the two structural families. Still, this equilibrium cannot account for the observed signal broadening, and the Asp4 NH/Hβ and Hα/Hβ distances in the calculated structures cannot reproduce the experimental values. Furthermore, the Asp4 $^3J_{\alpha\beta}$ coupling constants (see preceding paper in this issue) indicate that conformations with χ_1 near −80° (as in TUC4–TUC7, Table II) may be the most populated, but the coupling values observed can only be explained if other rotamers of the Asp4 side chain are significantly visited. The observation that the original value of Asp4 χ_1 in the unrestrained TU structure is −155° (Table II) suggested that an additional conformational interconversion involving this dihedral angle could be occurring. In order to explore this possibility, a 30-ps molecular dynamics trajectory at 600 K was calculated, starting from structure TUC6 and using no restraints on any proton of the Asp4 and Dpr10 side chains. The evolution of Asp4 χ_1 during the simulation (Figure 5c) shows that conformations with Asp4 χ_1 near −180° may indeed be interconverting with the restrained structures found previously. The energies of the new structures are similar to those of TUC6 and TUC7 (around 200 kcal/mol), and the overall shape of the molecule is preserved. All interproton distances around the bridge and the $^3J_{\alpha\beta}$ coupling constants can be justified if these structures are significantly populated and in equilibrium with a major population of the restrained structures obtained previously (data not shown). The Dpr10 χ_1 torsion angle remained near −65° in all the calculated structures.

It is very difficult, if not impossible, to characterize in detail a conformational equilibrium when more than two structures appear to be significantly populated and only averaged experimental parameters are available. Hence, it is very difficult to

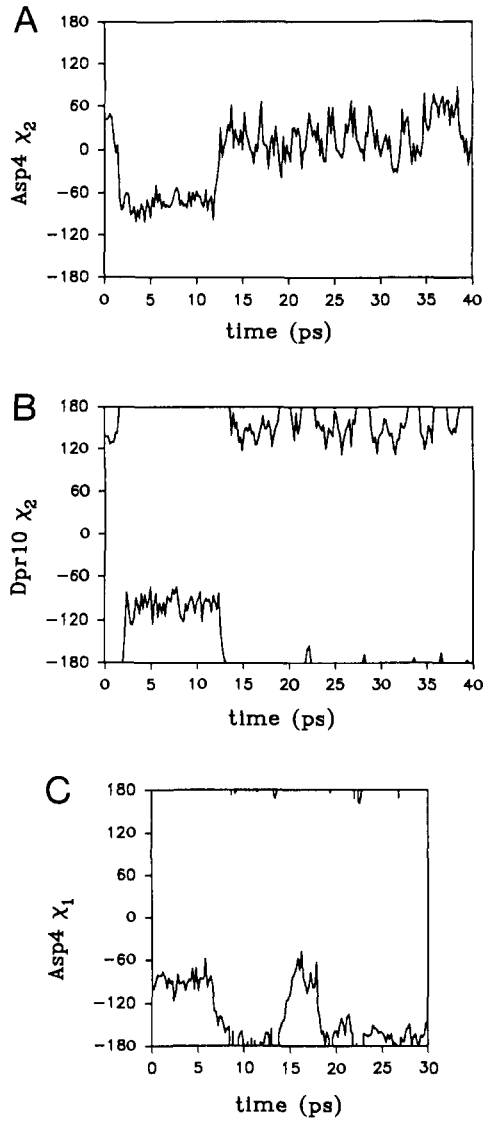

Figure 5. Evolution of some torsion angles in the Asp4–Dpr10 bridge in two molecular dynamics trajectories. Asp4 χ_2 (A) and Dpr10 χ_2 (B) as a function of time during the 40-ps, 300 K simulation that led to structures TUC4 and TUC5 (see text), illustrating a rotation around the central peptide bond of the bridge. (C) Variation of Asp4 χ_1 with time in a 30-ps, 600 K trajectory with no restraints on any proton of the Asp4 and Dpr10 side chains, started from TUC6 (see text); an interconversion between two rotameric states of the Asp4 side chain can be observed.

assess the accuracy of the conformations around the Asp4–Dpr10 bridge that have been obtained in the calculated structures, especially because of the lack of the solvent and of reliable restraints in this region of the molecule. For instance, the Dpr10 NH/NHγ restraint is well fit in some of the structures obtained, but the distance between these two protons increases to more than 3.7 Å when TUC6 and similar structures are minimized without this restraint. This may be correlated with a Dpr10 NH/Asp4 Oδ interaction, but this interaction is not observed by NMR and disappears when the solvent is included in the calculations (see below). Despite these considerations, our results enable us to formulate specific proposals for the motions that may contribute to the equilibria: a fast rotation around the Asp4 COδ/Dpr10 NHγ amide bond and a slow interconversion where Asp4 χ_1 changes between values around −70 and −90° and around −160 and −180°. The latter equilibrium, only observed in high-temperature molecular dynamics simulations, could be sufficiently slow in the experimental conditions to produce the observed signal broadening. Finally it is worth noting that the rms deviations for the backbone atoms in residues 5–8 that were obtained when several structures with different bridge conformation were compared ranged from 0.06 to 0.14 Å, indicating that the conformational equilibria can exist with small perturbation of the β-hairpin structure present on the other side of the ring.

Effect of the Environment. The molecular dynamics calculations described above have led to a refined conformational model for the Asp4–Dpr10 analogue, which can fit most experimental observations. However, the energy of structures that should be preferentially sampled according to the NMR data (TUC6–7, TDC4U) is about 25 kcal/mol higher than the energy of the original TU conformation and about 33 kcal/mol above the TD conformation (Table I). For the model to be reasonable from the theoretical point of view, the theory itself should afford an explanation for such high-energy differences. Three main factors must be considered in this context: the accuracy of the force field used to describe the molecule, the solvation energies of the different conformations, and the entropic contributions to the free energy of the system. The correctness of the force field is in fact one of the elements that we would like to assess, and the extent to which the other two factors may account for these energy differences using this force field should give an idea of its ability to reproduce experimental results on the system under study, as well as the importance of these effects themselves. In the ensuing analysis, we take the TUC6 conformation as representative of the structures incorporating the restraints, and we compare it with the nonrestrained TU and TD conformations.

In the process followed to obtain TUC6 from the TU conformation, the highest increase in energy occurred when the D-Phe2, D-Trp3, and D-2Nal6 side chains were forced to adopt the χ_1 = 60° rotameric state (Table I). This observation is somewhat puzzling because this is the preferred rotamer for the three side chains, according to the NMR data. A careful comparison of the TU and TUC6 structures (Figure 1) shows that the unrestrained structure has a much more compact shape, with the three aromatic side chains folded around the molecule; the restrained structure has a more extended appearance, with the three aromatic rings pointing outside the molecule. Indeed, this observation is not surprising. In calculations carried out in vacuo, the intramolecular nonbonding interactions will favor the maximally folded conformations allowed by the flexibility of the molecule. The large D-Phe2, D-Trp3, and D-2Nal6 side chains are interacting strongly with the rest of the molecule in the TU conformation, and part of these favorable interactions are broken when the aromatic rings are forced out of their folded orientations. In order to quantify these interactions, the total nonbonding energies in the TU and TUC6 conformations, and also the interresidue nonbonding energies involving D-Phe2, D-Trp3, and D-2Nal6, were calculated. For comparison, these energies were also calculated in the TD conformation, the lowest energy structure found in vacuo for the Asp4–Dpr10 analogue, which also presents a highly compact shape (Figure 1). To have a more quantitative estimate of the "compact" and "extended" attributes ascribed to these structures, their exposed surface area was calculated using the Connolly algorithm.[25] The results of these calculations are summarized in Table V, section A. The exposed surface area in the TUC6 conformation is clearly larger than in TU and TD. The differences in the computed nonbonding interactions in TU and TUC6, either considering the global values (difference 20.2 kcal/mol) or those corresponding to interresidue interactions involving residues 2, 3, and 6 (12.9 kcal/mol), are comparable to the energy increase observed when the three side chains were forced to adopt the preferred rotamers (energy TUC6–TUC6 = 16.6 kcal/mol, Table I). In fact, the interactions of residues 2, 3, and 6 with nonneighboring residues are 16.6 kcal/mol more favorable in TU, which confirms that a major contribution to the low energy of this conformation is due to its compact nature. We can also observe that the computed nonbonding energies are more favorable in the TD structure than in TU and TUC6, but the comparison is more difficult because of the large difference in the backbone conformation. The most important points to note are that a very significant stabilization of the TD conformation (about 10 kcal/mol) is due to van der Waals interactions between the stacked Tyr5 and D-2Nal6 aromatic side chains, and that the total non-

Table V. Thermodynamic Parameters and Exposed Surface Areas for Selected Conformations of the Asp4–Dpr10 Analogue[a]

A. In Vacuo Structures[b]

	TD	TU	TUC6
energy	166.5	174.0	199.5
nonbonding energy[c]	17.3	20.6	40.8
NBE (2, 3, 6)[d]	−95.7	−80.5	−67.6
NBE (2, 3, 6) nonneigh[e]	−56.7	−48.7	−32.1
vib entropy × T[f]	120.4	119.1	123.5[h]
vib free energy[f]	902.9	905.3	899.7[h]
exposed surface area[g]	893	892	1027

B. Solvent Systems[i]

	TD	TU	TUC6[m]
initial energy[j]	88.8	100.2	115.0
minimum energy[k]	88.1	95.1	107.9 (105.3[n])
	64.8[p]	63.6[p]	73.5[p] (71.2[n,p])
solvation energy in minimum[l]	−81.0	−84.3	−99.3 (−100.6[n])
	−109.0[p]	−116.9[p]	−134.8[p] (−136.1[n,p])
exposed surface area in minimum[g,k]	898	908	1074
rms minimum/in vacuo[q]	0.49	1.30	1.42

[a] Energy terms in kilocalories per mole. Exposed surface areas in squared angstroms. [b] Structures described in Tables I–III and Figure 1. [c] Total nonbonding energies (Coulomb + van der Waals) extracted from the total energies above. [d] Total interresidue nonbonding energies involving residues Phe2, Trp3, and 2Nal6. [e] Nonbonding energies involving residues Phe2, Trp3, and 2Nal6 when only interactions with nonneighbor residues are taken into account. [f] Vibrational free energy and entropy contribution at 300 K, calculated by vibrational normal mode analysis. [g] Total exposed surface areas calculated with the Connolly algorithm (ref 25). [h] Obtained on the TUC6 structure minimized without restraints (energy 195.9 kcal/mol; rms deviation with TUC6 conformation for all atoms 0.57 Å). [i] Solvent systems derived from the TD, TU, and TUC6 structures. All parameters given refer only to the Asp4–Dpr10 molecule in the system. [j] In structures obtained after solvating the in vacuo conformations with $CDCl_3$ and energy minimization. The energy values given correspond to intramolecular interactions in the Asp4–Dpr10 analogue molecule plus its interactions with the solvent. [k] In minimum energy structures obtained along the molecular dynamics trajectories. [l] Corresponding to intermolecular interactions of the Asp4–Dpr10 analogue molecule with the solvent. [m] Minimum energy structure (107.9 kcal/mol) is TUC6S in Tables I–III. [n] In structure obtained after further minimization without restraints (rms deviation with restrained minimum for all atoms 0.17 Å). [o] Obtained when the same instantaneous structures from the trajectories, which yielded the lowest energy minima, are minimized using the van der Waals parameters for chlorine described in ref 34. [q] Rms deviation (Å) for all atoms between the minimum energy structure in the solvent simulation and the original in vacuo structure.

bonding energies in TD are 23.5 kcal/mol more favorable than in TUC6. It is clear from these results that the nonbonding energies, especially those involving residues D-Phe2, D-Trp3, and D-2Nal6, make a major contribution to the differences observed in the total energies of the calculated structures. Thus, what might at first appear to be a highly strained structure storing considerable steric or deformation energy is actually an open structure containing "unsatisfied" van der Waals interactions. This is an important distinction to consider when comparing the energies in vacuo of different conformations of relatively flexible molecules.

Molecular Dynamics in Solvent. It is reasonable to assume that at least part of the nonbonding interactions lost when the side chains are forced onto the preferred rotameric states of the Asp4–Dpr10 analogue would be replaced by interactions with the solvent if it were included in the calculations. Hence, higher solvation energies are expected for the restrained structures, with respect to the TU and TD conformations. To estimate the solvation energies of different structures of the Asp4–Dpr10 analogue, and to study the effect of the solvent on its conformational behavior, a series of calculations was performed with the molecule embedded in a $CDCl_3$ bath. Three solvent systems were generated, with 297 $CDCl_3$ molecules and the Asp4–Dpr10 analogue in the TD, TU, or TUC6 conformation. The three systems were then energy minimized, a 30-ps molecular dynamics trajectory at 300 K was calculated for each of them, and six snapshots taken at 5-ps intervals along each trajectory were also energy minimized. Interproton distance and hydrogen-bonding restraints were maintained during the simulation and the minimizations for the solvent system including the TUC6 conformation and the restrained minima were further minimized without restraints. The most significant results obtained from these calculations are summarized below and in Table V, section B.[33]

No major changes in the overall conformations were observed along any of the molecular dynamics trajectories of the Asp4–Dpr10 analogue carried out in solvent. However, some meaningful differences were observed in the response of the different conformations to the presence of solvent in the calculations. The TD conformation showed the least sensitivity, with no significant change in any of the minimized structures with respect to the in vacuo conformation. The energy of the minima (intramolecular plus interactions with the solvent) oscillated between 88.1 and 94.3 kcal/mol and was in most cases higher than the energy of the starting solvated structure (88.8 kcal/mol). The lowest energy conformation, which occurred at 15 ps, is very similar to the in vacuo TD conformation (rms deviation for all atoms 0.49 Å) and has an almost identical exposed surface area (Table V). For the TU conformation, the most notable change in the molecular dynamics simulation in solvent occurred after 6 ps, when the Phe2 side chain rotated to populate the $\chi_1 = 60°$ rotameric state, the preferred one according to the NMR data. This change underlies the larger rms deviation observed between the in vacuo conformation and the minimum energy solvated structure, which occurs at 15 ps, and also causes an increase in the solvent exposed surface area (Table V). The decrease in the energy of the minimum energy conformation with respect to the starting solvated structure (5.1 kcal/mol) was much greater than in the TD conformation. These observations point to a greater sensitivity of the TU conformation to the environment.

The largest changes induced by the solvent were observed in the restrained simulation, starting from the solvated TUC6 conformation. While in the unrestrained simulations the minimum energy conformations occurred in the middle of the trajectory, in this simulation the energy decreased monotonically from the initial structure to the final conformation at 30 ps. The final structure (TUC6S, Tables I–III and Figure 1) has an rms deviation of 1.42 Å with respect to TUC6, and has a substantially larger exposed surface area (Table V). Both observations can be associated with a rotation of the D-Trp3 aromatic ring, where χ_2 changes from −153° to −96° to produce a higher exposure of this ring to the solvent, and with small rearrangements in other parts of the molecule. Some interesting differences in torsion angles and hydrogen-bonding patterns, arising from these rearrangements, are observed when the conformations in solvent, TUC6S, and in vacuo, TUC6, are compared. The ϕ and ψ dihedral angles of residues D-2Nal6 and Leu7 are considerably closer to those of an ideal type II′ β turn in TUC6S (Table II). Correspondingly, TUC6S lacks the hydrogen bond between Leu7 NH and Tyr5 CO, which closes a γ turn around D-2Nal6 and was present in most structures obtained in vacuo (Table III). Indeed, none of the hydrogen bonds between backbone atoms that were observed in the in vacuo conformations and were inconsistent with the amide temperature coefficients is found in the TUC6S structure (Table III). In calculations carried out in vacuo, it is usual to observe excessive hydrogen bonding, leading in many cases to the formation of γ turns. We can see that this tendency is highly alleviated with the presence of solvent in the calculations, even when the solvent is fairly apolar. It is also worth noting that while the restrained structure obtained in the solvent simulations –TUC6S– presents a better overall agreement with the NMR data than the in vacuo structure –TUC6–, the deviation with respect to the measured interproton distances is similar for both structures (Table I). The question is that, at the same time that the uncertainty in the interproton distances allows a natural flexibility

(33) A more detailed report on the molecular dynamics simulations in solvent will be published separately.

for the molecule, this flexibility can lead to significantly different torsion angles and hydrogen-bonding patterns within the same overall conformation. Our results show that the inclusion of solvent in the calculations leads to improved structures and correlate with those described by Lautz et al.[8]

As has been mentioned above, the largest decrease in energy on solvating the peptide (7.1 kcal/mol) occurred for the restrained structure, TUC6 (Table V). This energy decrease arises from a higher sensitivity to the environment, due to more efficient solvation of the structure. The conformational changes that led to TUC6S produced an increase of 7.7 kcal/mol in intramolecular energy with respect to TUC6 (Table I), but the additional intramolecular energy is more than compensated by the favorable solvation energy. An additional decrease in energy of 2.6 kcal/mol results when the TUC6S solvent system is further minimized without restraints (Table V, section B); the resulting structure is almost identical to TUC6S (0.17-Å rms deviation for all atoms), and the D-Phe2 NH/D-Trp3 NH distance is the only interproton distance that deviates significantly from the limits. As was predicted from the analysis of the energy contributions in TD, TU, and TUC6, the solvation energy is much more negative for the restrained (and extended) structure, and consequently, the energy differences between the solvated TUC6 structure and the solvated TD and TU conformations are much smaller than those observed in vacuo (Table V).

An accurate evaluation of the solvation energies is indispensable for a reliable comparison of the total energies of the Asp4–Dpr10 analogue conformations. In this context, the van der Waals parameters for Cl are major determinants of the solvation energies in $CDCl_3$, and those included in the DISCOVER force field have not been sufficiently tested, as Cl is not a common atom in peptides and proteins. To have another estimate of the energies of the solvent systems, the same instantaneous structures from the three trajectories that yielded the three minimum energy conformations were minimized with the same force field, but using the van der Waals parameters for Cl described by Giglio[34] (Table V, section B). More negative solvation energies are obtained with these parameters,[35] and hence, a further decrease of the relative energy of the solvated restrained structure with respect to the solvated TD and TU conformations is observed. Note that the solvation energy of the restrained structure, TUC6, can be up to 27 kcal/mol more favorable than in TD and also that, with these parameters, the unrestrained TU conformation has lower energy than the TD conformation (Table V, section B). The large differences in the solvation energies obtained with the different parameters indicate the necessity of further research to ascertain which are reliable van der Waals parameters for Cl and leave a high uncertainty in the relative energy of the solvated conformations of the Asp4–Dpr10 analogue. However, it is clear from our results that the stronger the solvation effect, the lower the relative energy of the restrained structure with respect to the unrestrained ones.

Entropic Considerations. To this point, we have only considered energy contributions to the free energy of different conformations of the Asp4–Dpr10 analogue. As the TD, TU, and TUC6 conformations differ substantially, it is reasonable to expect that entropic factors could contribute significantly to the differences in the free energy of these conformations.[24b] One might expect the low-energy, compact TD and TU conformations to be more restricted and have smaller conformational fluctuations (lower entropy) than the more open, extended TUC6 structure. To obtain some idea of the magnitude of these entropic factors, we performed a vibrational free energy analysis. These calculations must be carried out on minimized, stable conformations, and hence, they were performed on the TD, TU, and TUC6 structures after minimizing them to a maximum derivative less than 0.0001 kcal/(Å·mol). No restraints were used here to minimize the TUC6 conformation, and the resulting structure had an energy of 195.9 kcal/mol and a 0.57-Å rms deviation for all atoms with TUC6. The results (Table V, section A) indicate that, as expected, the entropic contribution to the free energy of the unrestrained TUC6 conformation in vacuo, at 300 K, is more negative than those of TU and TD (4.4 and 3.1 kcal/mol, respectively). Nevertheless, these results have been obtained in vacuo and represent only the conformational entropy of these structures. Larger entropic effects might appear if we could account for the total volume of phase space corresponding to the ensemble of structures compatible with our NMR/molecular dynamics analysis, and compare it with the phase space near conformations with energies as low as TU and TD. No such calculations have been pursued here, but we have initiated work in this direction.

The most important points that we would like to emphasize from our results are the following: (i) the energy difference between a restrained structure, TUC6, and the lowest energy conformation found in vacuo, TD, is 33.0 kcal/mol, but this difference can decrease to only 6.4 kcal/mol when solvent is included in the calculations; (ii) in solvent, the unrestrained tail-up minimum can have lower energy than the minimum with the tail down; (iii) local entropic effects favor the NMR structures by a few kilocalories per mole. To evaluate our results, a number of factors must be considered: the limited time of the simulations performed in solvent, the absence in these simulations of the cosolvent DMSO-d_6, indispensable to solubilize the Asp4–Dpr10 analogue in our experimental conditions, the uncertainty in the solvation energies calculated, and the limitations of the analysis of entropic factors. Despite these drawbacks, we can conclude that, for molecules of the size and flexibility of the Asp4–Dpr10 analogue, structures obtained in vacuo with energies more than 30 kcal/mol above the lowest energy conformation found may still be reasonable from the theoretical point of view when solvation energies and entropy contributions to the free energy are taken into account. This observation has important implications for modeling studies that are carried out without any experimental restraints and where the selection of conformations is mainly based on energetic grounds. Our results indicate that fundamental conformations of the target molecule, such as those observed experimentally, can be overlooked unless large energy thresholds are used for this selection. This is particularly important in studies of flexible molecules. Wherever there is flexibility in a molecule, in vacuo calculations will be strongly biased toward maximally folded, compact conformations. Although these structures still indicate conformational tendencies of the molecule that could be useful for analogue design, they may be difficult to obtain experimentally.

Design of New GnRH Antagonists. The ultimate goal of the work presented here is the design of new constrained GnRH antagonists with increased potency. Our molecular dynamics simulations led to two fundamentally different families of conformations, with the tail formed by residues 1–3 located above or below the ring. The lowest energy structure found in vacuo has the tail below the ring, and although the existence of this structure is not supported by our experimental data, there is no proof that this is not the actual conformation adopted by the Asp4–Dpr10 analogue upon binding to the GnRH receptor. Tail-up and tail-down conformations offer different bridging opportunities to design new GnRH analogues, and as long as no direct evidence for the actual binding conformation of GnRH or any of its active analogues is obtained, only the success in designing potent GnRH analogues based on one or another conformational hypothesis can confirm its validity.

The overall conformation found for the Asp4–Dpr10 analogue shows clear similarities with the structure of the parent cyclic decapeptide GnRH antagonist, cyclo(Δ^3-Pro1-D-*p*ClPhe2-D-Trp3-Ser4-Tyr5-D-Trp6-NMeLeu7-Arg8-Pro9-β-Ala10).[6,7,36] A

(34) Giglio, E. *Nature* **1969**, *222*, 339–341. These parameters have been successfully applied to the study of the influence of crystal forces on molecular conformation using *p*-(*N*-chlorobenzylidene)-*p*-chloroaniline as a model (Bernstein, J.; Hagler, A. T. *J. Am. Chem. Soc.* **1978**, *100*, 673–681).

(35) The minimum van der Waals energy radius for Cl in the DISCOVER force field is 3.970 Å, and the one given by E. Giglio is 3.866 Å; the depths of the potential energy well, ϵ, are −0.0691 and −0.244 kcal/mol, respectively. More negative solvation energies are expected for more negative values of ϵ. Current efforts in our laboratory are directed to assess the correctness of either value of ϵ.

(36) Baniak, E. L., II; Rivier, J. E.; Struthers, R. S.; Hagler, A. T.; Gierasch, L. M. *Biochemistry* **1987**, *26*, 2642–2656.

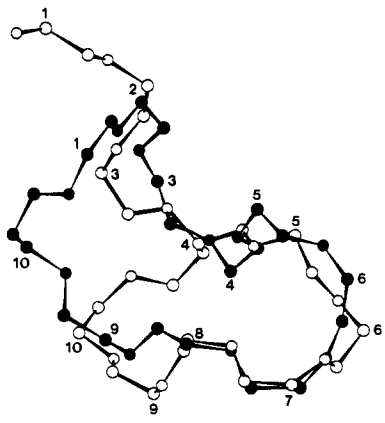

Figure 6. Superposition of the backbone atoms of the TUC6 conformation of the Asp4-Dpr10 analogue (○) and the structure determined for the parent cyclic decapeptide (●) (see text). The numbers indicate the positions of the Cα carbons.

β-hairpin structure involving residues 5–8 was also found for the cyclic decapeptide, and the backbone of residues 1–3 and 10 appeared to be oriented above the plane defined by the β-hairpin, in analogy with the orientation of the tail above the ring in the Asp4–Dpr10 analogue (Figure 6). There is also a type II′ β turn around residues 6 and 7 in both analogues, which has been proposed to be essential for biological activity. An interesting feature in most of the restrained structures obtained for the Asp4–Dpr10 analogue is the presence of numerous hydrogen-bonding interactions involving the side chains of Tyr5 and Arg8 and carbonyl groups in the tail (Table III), interactions that remained when solvent was included in the calculations. The persistence of these interactions may be due to the lack of the strong hydrogen bond acceptor DMSO-d_6 in the calculations, and to a limited sampling of the conformational space available to these side chains. However, these electrostatic interactions are intrinsically favored by the conformation of the molecule: due to the β-hairpin structure adopted by residues 5–8, both the Tyr5 and Arg8 side chains are oriented above the ring, on the same side where the tail is located.[37] The approach of the tail and these side chains in our proposed bioactive conformation offers very good bridging opportunities for the design of more constrained GnRH analogues. Indeed, bicyclic (4–10, 5–8) analogues of GnRH have already been synthesized and tested, and an antagonist that is equipotent to the Asp4–Dpr10 analogue has been developed.[38] We have recently prepared monocyclic GnRH analogues bridging the side chain in position 8 with either the N-terminus or the side chains of residues 1, 2, or 3, but no active analogues have been found as yet (unpublished). One may speculate that the 4–10 bridge is necessary to maintain the β turn around residues 6 and 7, and in these monocyclic compounds the turn may not be favored. Our results suggest that bicyclic compounds incorporating the 4–10 bridge and a linkage between positions 0/3 and residue 5 or 8 should be explored for the development of new GnRH antagonists with enhanced potency.

(37) Although no strong evidence for the presence of tail/Tyr5/Arg8 hydrogen bonds was obtained in our NMR data, some experimental observations suggest their likelihood. For instance, the Tyr5 side chain rotamer that brings about these interactions ($\chi_1 = 60°$) appears to be more populated than it is statistically observed in proteins. On the other hand, the Arg8 side chain in the restrained structures is directed toward the tail and Tyr5 in a natural, completely extended conformation. The observation of an Arg8 Hγ/Pro9 Hδ2 NOE indicates that this orientation of the Arg8 side chain is among those preferentially visited by this side chain (see preceding paper in this issue).

(38) Rivier, J. E.; Rivier, C.; Vale, W.; Koerber, S.; Corrigan, A.; Porter, J.; Gierasch, L. M.; Hagler, A. T. In *Peptides: Chemistry, Structure and Biology*; Rivier, E. J., Marshall, G. R., Eds.; ESCOM: Leiden, The Netherlands, 1990; pp 33–37.

Summary

The conformational model of the Asp4–Dpr10 GnRH analogue delineated from our NMR analysis (see preceding paper in this issue) has been refined by molecular dynamics simulations. Two main families of structures, with the tail above or below the ring, were obtained in an initial conformational search without restraints. Application of NMR restraints to both conformational families distinguished between the two and led to tail-up structures as those consistent with the NMR data. The experimental data also predicted a β-hairpin conformation in residues 5–8 which is adopted by the molecule in the restrained simulations with a moderate strain energy. The simulations indicate the presence of two different conformational equilibria localized in the Asp4–Dpr10 bridge that help to rationalize the NMR observations. The existence of a γ turn around D-Trp3, closed by a hydrogen bond between Asp4 NH and D-Phe2 CO and previously suggested from the NMR data, is supported by the simulations, which also indicate that Dpr10 NHγ can be hydrogen bonded to D-Trp3 CO for some conformations of the bridge. A high mobility in residues 1 and 2 is confirmed, with indications that a type II β-turn conformation around these residues may be visited frequently. The presence of numerous tail/Tyr5/Arg8 interactions in the calculated structures suggests new bridging constraints that could be introduced in the molecule to obtain more rigid GnRH antagonists. Bicyclic analogues that have already been synthesized to incorporate some of these constraints present variable degrees of biological activity, which indicate that the structures obtained for the Asp4–Dpr10 analogue should be closely related to its bound conformation.

The molecular dynamics study of the Asp4–Dpr10 GnRH analogue presented here underlines the difficulties associated with the conformational analysis of molecules with some flexibility. Only a careful choice of interproton distance restraints could yield realistic structures and help to elucidate the conformational behavior of the molecule. In calculations carried out in vacuo, the nonbonding interactions can easily dominate the energy differences between conformations, especially when large aromatic side chains are present. Hence, well-packed, compact structures will be highly favored in vacuo, while conformations that fit the experimental data can be of significantly higher energy (about 30 kcal/mol for molecules with the size of the Asp4–Dpr10 analogue). The "unsatisfied" nonbonding interactions leading to these high energies should be distinguished from actual valence or steric strain induced in the molecular structure in order to fit the restraints. The use of energy thresholds above the lowest energy structure found in a conformational search to consider the acceptability of a structure can be highly misleading unless the different contributions to the total energy are analyzed in detail. The inclusion of solvent in the calculations after a careful analysis of results obtained in vacuo can lead to improved structures for the target molecule and help to better understand its energetics and conformational characteristics.

Acknowledgment. We thank Ron Kaiser, John Porter, Duane Pantoja, and Charleen Miller for technical assistance in the synthesis and characterization of the Asp4–Dpr10 GnRH analogue. J.R. was a fellow from the Ministerio de Educación y Ciencia of Spain. This work was supported by NIH Contract No. NO1-HD-1-3100 and by a Grant from the NIH (GM-27616 to L.M.G.). L.M.G. thanks the Robert A. Welch Foundation for continued support. Supercomputer time was provided by the San Diego Supercomputer Center (San Diego, CA) and by the Center for High Performance Supercomputing (Austin, TX).

Registry No. Asp4-Dpr10 analogue, 109001-26-5.